



Preventive Role of Hilar Parasympathetic Ganglia on Pulmonary Artery Vasospasm in Subarachnoid Hemorrhage: An Experimental Study

Subaraknoid Kanamada Hilar Parasempatik Ganglionun Pulmoner Arter Vazospazmı Üzerindeki Önleyici Rolü: Deneysel Bir Çalışma

Omer ARAZ¹, Mehmet Dumlu AYDIN², Betül GUNDOGDU³, Ender ALTAS⁴, Murteza ÇAKIR², Çagatay CALIKOGLU², Canan ATALAY⁵, Cemal GUNDOGDU³

¹Ataturk University, School of Medicine, Department of Pulmonary Diseases, Erzurum, Turkey

²Ataturk University, School of Medicine, Department of Neurosurgery, Erzurum, Turkey

³Ataturk University, School of Medicine, Department of Pathology, Erzurum, Turkey

⁴Palandoken Government Hospital, Department of Cardiology, Erzurum, Turkey

⁵Ataturk University, School of Medicine, Department of Anesthesiology and Reanimation, Erzurum, Turkey

Corresponding Author: Mehmet Dumlu AYDIN / E-mail: nmda11@hotmail.com

ABSTRACT

AIM: Pulmonary arteries are mainly innervated by sympathetic vasoconstrictor and parasympathetic vasodilatory fibers. We examined whether there is a relationship between the neuron densities of hilar parasympathetic ganglia and pulmonary vasospasm in subarachnoid hemorrhage (SAH).

MATERIAL and METHODS: Twenty-four rabbits were divided into two groups: control (n=8) and SAH (n=16). The animals were observed for 20 days following experimental SAH. The number of hilar parasympathetic ganglia and their neuron densities were determined. Proportion of pulmonary artery ring surface to lumen surface values was accepted as vasospasm index (VSI). Neuron densities of the hilar ganglia and VSI values were compared statistically.

RESULTS: Animals in the SAH group experienced either mild (n=6) or severe (n=10) pulmonary artery vasospasm. In the control group, the mean VSI of pulmonary arteries was 0.777 ± 0.048 and the hilar ganglion neuron density was estimated as $12.100 \pm 2.010/\text{mm}^3$. In SAH animals with mild vasospasm, $\text{VSI}=1.148 \pm 0.090$ and neuron density was estimated as $10.110 \pm 1.430/\text{mm}^3$; in animals with severe vasospasm, $\text{VSI}=1.500 \pm 0.120$ and neuron density was estimated as $7.340 \pm 990/\text{mm}^3$.

CONCLUSION: There was an inverse correlation between quantity and neuron density of hilar ganglia and vasospasm index value. The low numbers and low density of hilar parasympathetic ganglia may be responsible for the more severe artery vasospasm in SAH.

KEYWORDS: Hilar parasympathetic ganglion, Neuron density, Pulmonary artery vasospasm, Subarachnoid hemorrhage, Rabbit

ÖZ

AMAÇ: Pulmoner arterlerin ana inervasyonunu sempatik vazokonstriktör ve parasempatik vazodilatör lifler tarafından yapılır. Biz subaraknoid kanamada (SAK) pulmoner arter vazospazmı ile hilar parasempatik ganglionun nöron dansitesi arasındaki ilişkiyi değerlendirdik.

YÖNTEM ve GEREÇLER: Yirmi dört tavşan iki gruba bölündü: 8'i kontrol ve 16'sı SAK oluşturulan gruptu. Hayvanlar 20 gün boyunca takip edildi. Hilar parasempatik ganglion sayıları ve nöron dansiteleri tespit edildi. Pulmoner arterin dış çapı ile iç yüzey çapı oranı vazospazm indeksi olarak (VSI) kabul edildi. Nöron dansitesi ile VSI istatistiksel olarak karşılaştırıldı.

BULGULAR: SAK grupta altı hayvanda hafif, 10 hayvanda şiddetli vazospazm tespit edildi. Kontrol grubunda tahmini olarak hilar ganglion nöron dansitesi $12,100 \pm 2,010/\text{mm}^3$ ve VSI $0,777 \pm 0,048$ olarak tespit edildi. Yine hafif derecede pulmoner arter vazospazmı olan SAK'lı grupta hilar ganglion nöron dansitesi $10,110 \pm 1,430/\text{mm}^3$ ve VSI $1,148 \pm 0,090$, şiddetli spazmı olan grupta ise hilar ganglion nöron dansitesi $7,340 \pm 990/\text{mm}^3$ ve VSI $1,500 \pm 0,120$ tahmini olarak tespit edildi.

SONUÇ: Hilar ganglion nöron dansitesi ile vazospazm indeksi arasında ters ilişki vardır. Subaraknoid kanamada az sayıda ve düşük dansitesi olan parasempatik ganglionlar şiddetli pulmoner arter vazospazmının sebebi olabilirler.

ANAHTAR SÖZCÜKLER: Hilar parasempatik ganglion, Nöron dansitesi, Pulmoner arter vazospazmı, Subaraknoid kanama, Tavşan

INTRODUCTION

The most serious complication of SAH is pulmonary hypertension resulting from increased pulmonary vascular resistance (24). Pulmonary vasospasm is the most important mechanism in the development of pulmonary vascular resistance. The predominant pathology of increased pulmonary resistance is narrowed lumen resulting from vascular remodeling, excessive cell proliferation, reduced apoptosis and thrombus formation (15, 17, 20).

The diameter of pulmonary arteries is regulated by vasoconstrictor sympathetic nerves originating from cervical-thoracic sympathetic ganglia, vasodilatory parasympathetic vagal fibers and thoracic spinal afferent and efferent nerves. These nerves reach pulmonary tissue and vasculature via the pulmonary plexuses, which are formed by several large branches of the vagal nerve joined by smaller sympathetic nerves. These smaller sympathetic pulmonary nerves are comprised of the axons of postganglionic sympathetic fibers. The pulmonary plexus divides after entering the lung, and the nerves branch off to accompany the main bronchi and bronchial arteries. No plexus formation is found around these structures; instead, the nerve bundles wind around them and branch off at irregular intervals (12, 18)

All neurons generate electrical impulse when exposed to ischemic conditions, and electrical stimulation of vagal nerves causes pulmonary artery constriction (6,14). Therefore, ischemic injury sustained by the vagal nerve during subarachnoidal hemorrhage can cause cardiac arrest. Furthermore, lesions to the parasympathetic pathways trigger pulmonary vasospasm and pulmonary edema (2). Hypoxia develops in conjunction with these events, and this induces further vasoconstriction and inhibits immune response in the pulmonary tissue (5, 23).

We hypothesized that hilar parasympathetic ganglia have an essential role in the regulation of pulmonary circulation and pulmonary vessel diameter, as the vagal nerve network does. We examined the possibility that low hilar ganglia number or neuron density would correspond to greater severity of pulmonary artery vasospasm in the event of subarachnoid hemorrhage.

MATERIAL and METHODS

This study included 24 rabbits that had been used in previous experiments in our laboratory. The protocols for animal use were approved by the Ethics Committee of Atatürk University, Medical Faculty. The care of the animals and the experiments themselves were conducted according to the guidelines set forth by the same ethics committee. This study was also conducted in accordance with the National Institute of Health's Guide for the Care and Use of Laboratory Animals.

Experimental Procedure: General anesthesia with isoflurane was delivered by face mask, after which 0.2 mL/kg of the anesthetic combination (Ketamine HCl, 150 mg/1.5 mL; Xylazine HCl, 30 mg/1.5 mL; and distilled water, 1 mL)

was injected subcutaneously prior to surgery. During the procedure, 0.1 mL/kg doses of the anesthetic combination were administered as required. To create the experimental subarachnoid hemorrhage, an autologous blood sample (1 mL) was taken from the auricular vein and injected with a 22G needle into the cisterna magna of animals in the SAH group over the course of one minute. Animals in the control group were not subjected to the procedure. All animals were observed for 20 days with no medical treatment, and then sacrificed. Four animals died during the procedure or follow-up period, which were replaced with new subjects. The bodies of all animals were stored intact in 10% formalin solution after required preparatory procedures for future histologic analysis.

Animal selection: Pulmonary tissue samples were taken from 24 rabbits that had been used in a previous SAH study in our laboratory. Eight of the animals belonged to the control group and the remaining animals (n=16) were from the experimental SAH group.

Histopathological Procedures: To estimate the numbers of parasympathetic ganglia, the vagal nerves and their ganglia were examined under high magnification and excised bilaterally from the lung hilar, together with perihilar lung tissue. The samples were then longitudinally embedded in paraffin blocks for observing the vagal nerve axons and vagal parasympathetic ganglia neurons. Stereological and Cavalieri methods were used to estimate the neuron density of the hilar vagal ganglia. This approach reliably estimates particle number, can be readily performed, is intuitively simple, is free from assumptions about particle shape, size and orientation, and is unaffected by overestimation error of neuron numbers of the hilar ganglion or truncation. Two consecutive sections (dissector pairs) obtained from reference tissue samples were mounted on each slide. The paired reference sections were reversed in order to double the number of dissector pairs without requiring new sections. The mean numerical density of normal and degenerated neurons in the hilar ganglion (Nv/Gv) per cubic millimeter was estimated using the following formula.

$$Nv/Gv = \Sigma Q^{-}N / \Sigma A \times d$$

Where $\Sigma Q^{-}N$ is the total number of counted neurons appearing only in the reference sections, Nv : Normal neuron density, Gv : Degenerated neuron density, d is the section thickness, and A is the area of the counting frame. The most effective way of estimating ΣA for the set of dissectors is using $\Sigma A = \Sigma Pa$, where ΣP is the total number of counting set frame points and a is a constant area associated with the set point (13). The physical dissector stereological method was used to evaluate the number of neurons in the hilar ganglia and vagus nerve axon determination procedures. The Cavalieri method of volume estimation was used to determine the total number of neurons in each specimen by multiplying the volume (mm^3) of each hilar ganglion with its neuron density (11). Hilar ganglion neurons were quantified for each animal in the study (Figure 3 A, B).

Pulmonary arteries (PAs) were obtained from longitudinal lung sections taken 5 mm from the hilum. Then, 20 histopathologic sections, 5 μm apart, were obtained by microtome and are represented by the lines 1 through 20. The sections were stained with H&E. The mean external and internal (luminal) diameters of each section were measured; the external radius was represented as **R** and internal radius was represented as **r**. The mean radius values of pulmonary arteries were calculated as $R = (R_1 + R_2 + R_3 + \dots + R_{20})/20$; and the same method was used with **r** values to calculate mean lumen radius. The luminal area and wall thickness were calculated with the formulas $S_2 = \pi r^2$ and $S_1 = \pi R^2 - \pi r^2$, respectively. The vasospasm index (VSI) was calculated as the proportion of S_1/S_2 . Fully expanded, $VSI = S_1/S_2 = (\pi R^2 - \pi r^2)/\pi r^2 = \pi(R^2 - r^2)/\pi r^2 = (R^2 - r^2)/r^2$.

In summary, $VSI = (R^2 - r^2)/r^2$

Statistical Analysis

The data were analyzed using a commercially available statistics software package (SPSS® for Windows v. 17.0, Chicago, USA). Survival analysis was calculated by the Kaplan-Meier method, and then compared using the Log-rank test. The differences between the VSI values and neuron densities of the hilar ganglia were compared using the Mann-Whitney U test, with significance at $p < 0.05$.

RESULTS

Clinically, meningeal irritation signs, convulsions, fever, apnea, cardiac arrhythmia and breathing disturbances were observed in the premortal period of the three animals which died of severe SAH.

Baseline readings were taken from all animals, both in the control group and the SAH prior to surgery. The mean baseline heart rate (HR) was 250 ± 30 /min, respiratory rate (RR) was 30 ± 7 bpm and blood oxygen saturation (SO₂) was $95 \pm 5\%$. At onset of SAH, HR decreased to 140 ± 40 /min; RR was 15 ± 5 bpm and SO₂ was $70 \pm 10\%$. Considerable electrocardiographic changes were observed, such as ST depression, ventricular extrasystoles, bigeminal pulses, QRS separation and fibrillations. Immediately following SAH, RR was 20 ± 4 bpm; at the first follow-up 10 hours later, RR had increased to 40 ± 9 bpm with severe tachypneic and apneic variability. In the analysis of respiratory parameters, decreased respiration frequency (bradypnea; 15 ± 5 bpm) and increased respiration amplitude (30%) were observed in the first hours of SAH. Later, increased respiration frequency (tachypnea) and decreased respiration amplitude ($30 \pm 8\%$), shortened inspiration and extended expiration times, apnea/tachypnea attacks, diaphragmatic breathing and respiration arrest were observed. In the final stage of fatal SAH (Figure 1A,B), HR increased to 294 ± 30 /min and disordered respiration rhythm was detected as 38 ± 9 bpm compared to the animals' baseline RR of 30 ± 7 bpm. One of the animals died during procedure and the others on 2, 6 and 7 days.

The appearance of a vagal nerve with its hilar ganglia as seen in low magnification is shown in Figure 2. The number of

parasympathetic hilar ganglia was approximately 8 ± 1.3 per hilum. In control animals, this number was approximately 8.5 ± 1 ; in animals with mild vasospasm, 8.8 ± 1.4 ; in animals with severe vasospasm, 7.2 ± 0.9 . The stereological method of estimating neuron density of the hilar ganglia is illustrated in Figure 3A, B. The mean neuron density of hilar ganglia in both groups combined was estimated to be $9.600 \pm 2.560/\text{mm}^3$.

To estimate the VSI of PAs by stereological method, gridded glass plates were used while photographs were taken under microscope during histopathological examination. The inner elastic membrane (IEM) was less convoluted and the luminal surface area greater in the control and mild vasospastic SAH groups. PA narrowing, IEM convolutions, intimal edema formations and endothelial cell shrinkage, desquamation and endothelial cells loss were observed in the SAH group.

Animals in the SAH group developed either mild ($n=6$) or severe ($n=10$) pulmonary artery vasospasm. The mean VSI

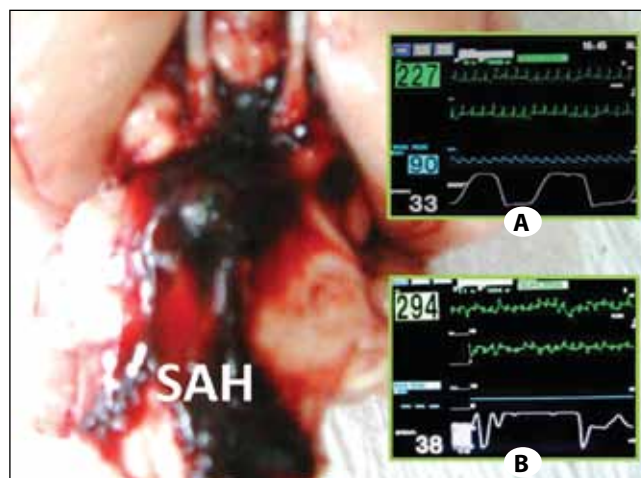


Figure 1: Macroscopic appearance of a brain with SAH, and **A)** Normal neuron density animal, **B)** Low neuron density animal EKG monitorization findings with respiration patterns.

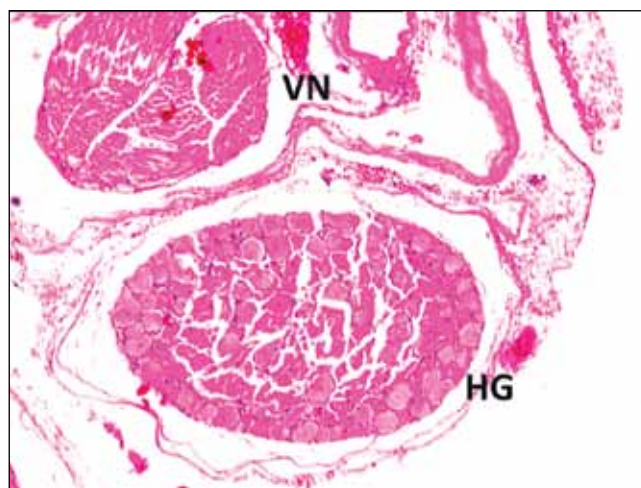


Figure 2: Vagal parasympathetic hilar ganglia (HG) and vagal nerve (VN) branch are shown (LM, H&E, x20).

of pulmonary arteries was 0.777 ± 0.048 and hilar ganglion neuron density was estimated as $12.100 \pm 2.010 / \text{mm}^3$ in control animals (Figure 4). In animals with mild vasospasm, the mean VSI of pulmonary arteries was 1.148 ± 0.090 and hilar ganglion neuron density was estimated as $10.110 \pm 1.430 / \text{mm}^3$ (Figure 5). However, in animals with severe vasospasm, the mean VSI of pulmonary arteries was 1.500 ± 0.120 and hilar ganglion neuron density was estimated as $7.340 \pm 990 / \text{mm}^3$ (Figure 6). All values are shown in Table I. Massive intraparenchymal lung

hemorrhage was noticed in severe pulmonary vasospasm developed two animals (Figure 7).

There was a significant difference in VSI values ($p < 0.001$) and hilar ganglion neuron densities ($p = 0.001$) between control and SAH groups; however, the number of hilar ganglia were not significantly different ($p = 0.145$). Survival analysis was calculated by the Kaplan-Meier method, and then compared using the Log-rank test (Figure 8) but there was no statistical significance ($p = 0.248$).

Table I: The Relationship between the Degenerated Vagal Ganglion Neuron Density and the Severity of Pulmonary Artery Vasospasm

	Normal Values	Mild Vasospasm	Severe Vasospasm
Normal ganglion density (neurons/ mm^3)	12.100 ± 2.010	10.110 ± 1.430	7.340 ± 990
Degenerate ganglion density (neurons/ mm^3)	26 ± 3	4.200 ± 550	9.100 ± 3.060
VSI	0.777 ± 0.048	1.148 ± 0.090	1.500 ± 0.120

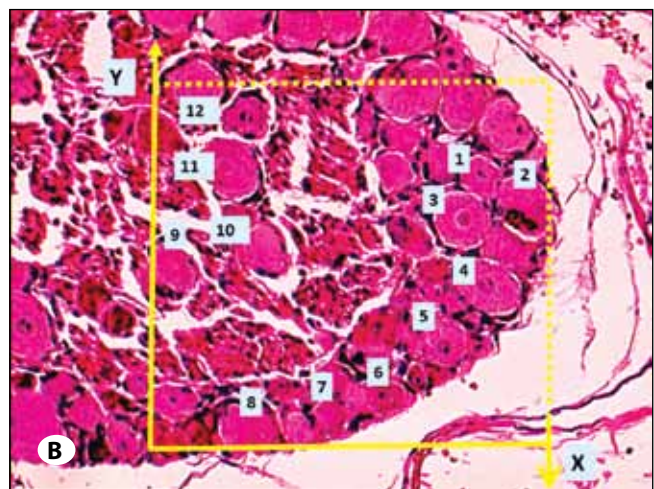
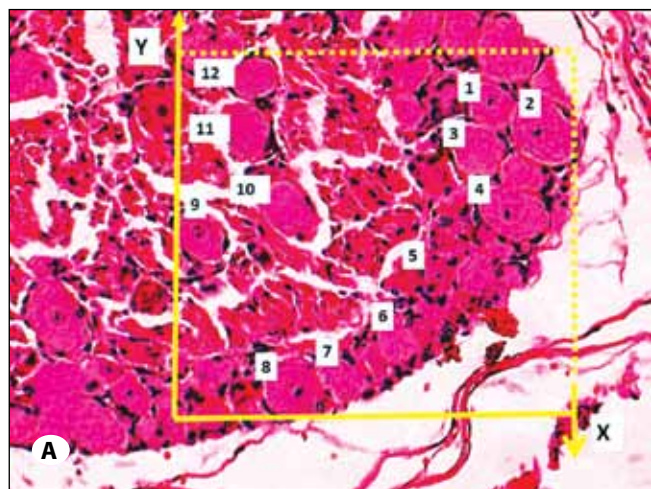


Figure 3 A, B: Stereologic cell counting of the hilar parasympathetic ganglia in a rabbit. In this application, the nucleoli marked with '4, 6-10' are disector particles in A. Section B shows them as they disappeared. The nucleoli marked with '1-3, 5' are not disector particles in A. Section B shows they are disappeared (LM, H&E, x200).

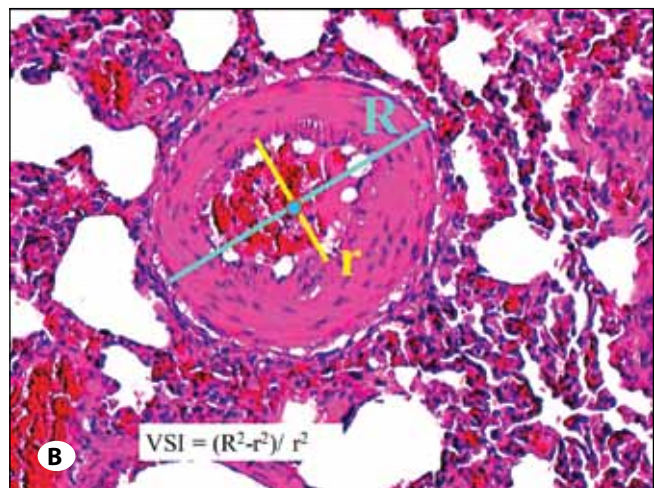
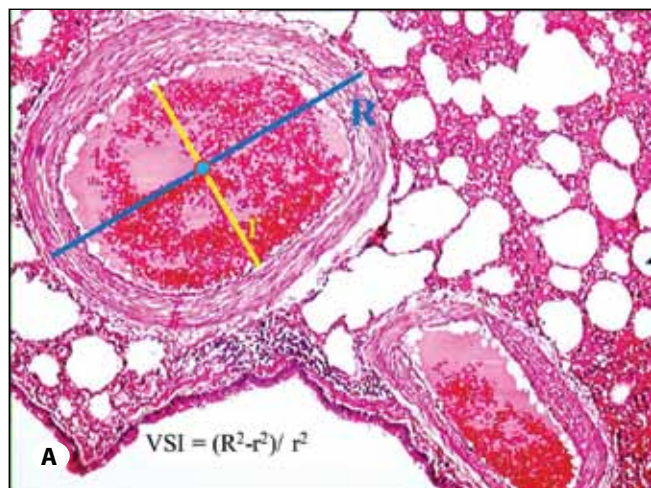


Figure 4: Histological view of a normal pulmonary artery (LM, H&E, x40).

Figure 5: Histopathological view of a pulmonary artery with mild vasospasm (LM, H&E, x40).

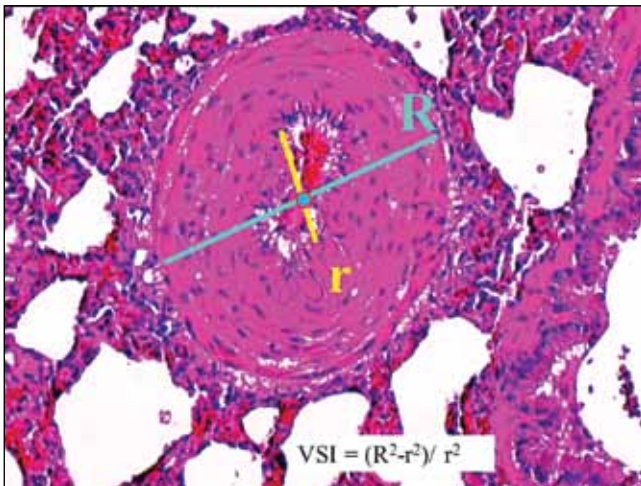


Figure 6: Histopathological view of a pulmonary artery with severe vasospasm (LM, H&E, x40).

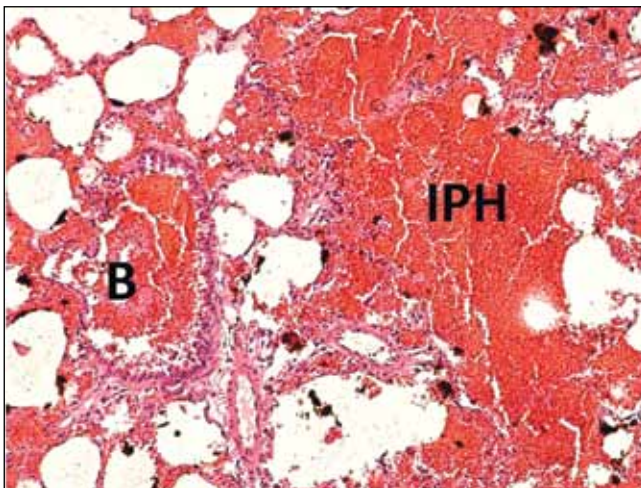


Figure 7: Intrapulmonary hemorrhage (IPH) was detected in some animals with fatal progressed SAH (LM, H&E, x40) (B: Bronchial).

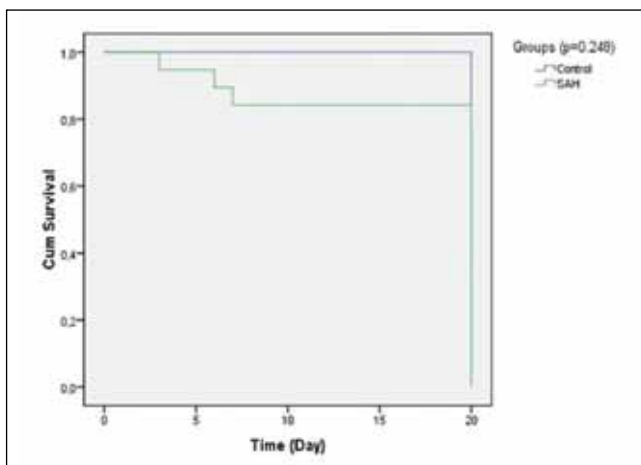


Figure 8: Survival analysis by Kaplan-Meier method, and comparison with Log-rank test ($p=0.248$).

DISCUSSION

Our findings can be summarized as follows: SAH resulted in vagal nerve ischemia at the brainstem due to vasospasm in arteries supplying both the afferent and efferent vagal nerve roots. Lower vagal axon densities corresponded with greater severity of vasospasm in animals in the SAH group, suggesting that degenerated vagal axons may play a major role in the development of pulmonary artery vasospasm.

Pulmonary hypertension (PHT) is an increase in the mean pulmonary arterial pressure at rest or exercise, with dyspnea on exertion being the most common presenting symptom. PHT is usually a progressive and ultimately fatal disease (3). While there are several possible underlying causes of PHT, all of the subtypes are characterized by excessive pulmonary vasoconstriction, as well as abnormal vascular remodeling processes affecting all vessel layers. These events result in severe luminal narrowing and increased right ventricular afterload (22). Reduced compliance in large pulmonary arteries also contributes to the strain on the right ventricle (8). Right ventricular hypertrophy (RVH) develops in response to the strains of increased pulmonary resistance. In RVH, muscle mass accumulates, the ventricle wall thickens, and the right ventricle assumes a more rounded shape, which compresses the left ventricle. Cardiac hypertrophy develops in PAH as a compensatory mechanism, allowing cardiac output to remain stable in the short term. However, progressive contractile dysfunction eventually occurs, leading to decompensation, dilatation, and right heart failure (4).

Pulmonary arteries are innervated by branches of the vagal nerve, sympathetic nerves and thoracic somatic nerves. All of these nerves form pulmonary ganglia composed of excitatory cholinergic neurons and inhibitory noradrenergic neurons and somatosensitive neurons, and they control the calibers of conducting airways, the diameter of pulmonary vasculature, the volume of respiratory units, the activity of bronchial glands and respiration reflexes. Vagal nerves are primarily responsible for the continuation pulmonary reflexes (7). Sensory innervation of the lower respiratory tract is thought to originate primarily from the nodose and jugular ganglia of the vagus nerve, C2-C6 and T1-T6 spinal ganglia. For rat pulmonary tissue, it has been shown that the sensory innervation mainly originates from the dorsal root ganglia (21).

The pulmonary plexuses are formed by several large branches of the vagal nerve joined by smaller sympathetic nerves. These smaller sympathetic pulmonary nerves are comprised of the axons of postganglionic sympathetic fibers, and they also contain afferent nerves. They run primarily to the posterior pulmonary plexus, but also contribute to the anterior pulmonary plexus. They join with branches of the vagal nerve and they together innervate the bronchi, vessels and pulmonary glands. Stimulating the cervical sympathetic trunk in the caudal direction induced vasoconstriction in the bronchial and pulmonary vasculature in control pigs (9).

Vagal nerve injuries can cause laryngopharyngeal muscle paralysis, tracheobronchial distortions, reflex vagal bradycardia and bradypnea (19). Vagal block diminishes both the frequency and amplitude of spontaneous breaths and vagal reactivity increases peripheral airway resistance during inspiration (10, 16). In late stage SAH, irreversible axonal injury of the vagal nerve may mimic vagal block (1). In SAH, first three week-period is very important because rebleeding, severe vasospasm, brain edema and herniation, ischemic neurodegenerative changes of lower cranial parasympathetic nerve ganglia can aggravate pulmonary vasospasm via directly decreased parasympathetic and relatively increased sympathetic overactivity.

In this study, the mechanisms that underlie the formation of pulmonary edema in SAH were also investigated. SAH caused vagal nerve injury, which led to degeneration in vagal ganglia and nerve branches that innervate the pulmonary tissue, resulting in mild to severe vasospasm. The degree of vasospasm is proportionate to the injury in the ganglia – the more damage, the more severe the vasospasm. Therefore, hilar parasympathetic ganglia injury affects blood flow to the pulmonary tissue through pulmonary artery vasospasm and results in right ventricle overload, which leads to left heart dysfunction. Overall, this plays an important role in the development of acute pulmonary edema. The mild form of pulmonary edema that develops immediately following SAH progresses to a more severe form in parallel to the progression of vagal nerve degeneration.

When we analyzed the animals, which their monitorization findings were accepted normal before SAH, after SAH, it was found that the animals with severe clinic had less ganglion number and neuron density. There was a negative correlation between neuron density and vasospasm degree. In the study of Aydin et al. (2), they found that SAH consecutively caused ischemic damage on vagal neuronal complex, denervation injury of hilar ganglia and then parasympathetic inhibition indirectly (10, 16, 21). This inhibition also increases vasospasm degree.

CONCLUSIONS

In conclusion, the parasympathetic vasodilatory impulses of vagal nerves have a major role in the maintenance of PA circulation under normal conditions. Ischemic injury of vagal nerve complexes induced by SAH can block parasympathetic pulmonary and cardiac control. This pathophysiologic process indirectly brings about sympathetic hyperactivity. Decreased parasympathetic and increased sympathetic impulses trigger the development of both massive pulmonary edema and depleted cardiac reserves. We propose that subcutaneous vagal nerve blocks may be useful at the beginning of SAH, whereas vagal nerve stimulation or sympathetic nerve blocks may be useful at the late phases of SAH.

REFERENCES

1. Aydin MD, Eroglu A, Turkyilmaz A, Erdem AF, Alici HA, Aydin N, Altas S, Unal B: The contribution of chemoreceptor-network injury to the development of respiratory arrest following subarachnoid hemorrhage. *EAJM* 42: 47-52, 2010
2. Aydin MD, Kanat A, Yilmaz A, Cakir M, Emet M, Cakir Z, Aslan S, Altas S, Gundogdu C: The role of ischemic neurodegeneration of the nodose ganglia on cardiac arrest after subarachnoid hemorrhage: An experimental study. *Exp Neurol* 230: 90-95, 2011
3. Barst RJ, McGoon M, Torbicki A, Sitbon O, Krowka MJ, Olschewski H, Gaine S: Diagnosis and differential assessment of pulmonary arterial hypertension. *J Am Coll Cardiol* 43: 405-407, 2004
4. Bogaard HJ, Abe K, Vonk Noordegraaf A, Voelkel NF: The right ventricle under pressure: Cellular and molecular mechanisms of right-heart failure in pulmonary hypertension. *Chest* 135: 794-804, 2009
5. Cairns RA, Hill RP: Acute hypoxia enhances spontaneous lymph node metastasis in an orthotopic murine model of human cervical carcinoma. *Cancer Res* 64: 2054-2061, 2004
6. Costa C, Tozzi A, Luchetti E, Siliquini S, Belcastro V, Tantucci M, Picconi B, Ientile R, Calabresi P, Pisani F: Electrophysiological actions of zonisamide on striatal neurons: Selective neuroprotection against complex I mitochondrial dysfunction. *Exp Neurol* 221: 217-224, 2010
7. Crapo JD, Barry BE, Czeahr P, Bachofen M, Weibel ER: Cell number and cell characteristics of the normal human lung. *Am Rev Respir Dis* 126: 332-333, 1982
8. Fourie PR, Coetzee AR, Bolliger CT: Pulmonary artery compliance: Its role in right ventricular-arterial coupling. *Cardiovasc Res* 26:839-844, 1992
9. Franco-Cereceda A, Matran R, Alving K, Lundberg JM: Sympathetic vascular control of the laryngeal-tracheal, bronchial and pulmonary circulation in the pig: Evidence for non-adrenergic mechanisms involving neuropeptide Y. *Acta Physiol Scand* 155: 193-204, 1995
10. Fuller SD, Freed AN: Partitioning of pulmonary function in rabbits during cholinergic stimulation. *J Appl Physiol* 78: 1242-1249, 1995
11. Gardi JE, Nyengaard JR, Gundersen HJG: The proportionator: Unbiased stereological estimation using biased automatic image analysis and non-uniform probability proportional to size sampling. *Comput Biol Med* 38: 313-328, 2008
12. Gross NJ, Skorodin MS: Anticholinergic, antimuscarinic bronchodilators. *Am Rev Respir Dis* 129: 856-870, 1984
13. Gundersen HJG: Notes on the estimation of the numerical density of arbitrary profiles: The edge effect. *J Microsc* 111: 219-223, 1977
14. Ikomi F, Kousai A, Ono N, Ohhashi T: Electrical stimulation-induced alpha1- and alpha2-adrenoceptors-mediated contractions of isolated canine lymph nodes. *Auton Neurosci* 96: 85-92, 2002
15. Lee SH, Rubin LJ: Current treatment strategies for pulmonary arterial hypertension. *J Int Med* 258: 199-215, 2005

16. Matsumoto S, Takeda M, Saiki C, Takahashi T, Ojima K: Effects of vagal and carotid chemoreceptor afferents on the frequency and pattern of spontaneous augmented breaths in rabbits. *Lung* 175: 175-186, 1997
17. Rich S, Kaufmann E, Levy PS: The effect of high doses of calcium-channel blockers on survival in primary pulmonary hypertension. *N Engl J Med* 327: 76-81, 1992
18. Richardson J, Béland J: Nonadrenergic inhibitory nervous system in human airways. *J Appl Physiol* 41:764-771, 1976
19. Ryan S, McNicholas WT, O'Regan RG, Nolan P: Effect of upper airway negative pressure and lung inflation on laryngeal motor unit activity in rabbit. *J Appl Physiol* 92: 269-278, 2002
20. Sitbon O, Humbert M, Jaïs X, loos V, Hamid AM, Provencher S, Garcia G, Parent F, Hervé P, Simonneau G: Long-term response to calcium channel blockers in idiopathic pulmonary arterial hypertension. *Circulation* 111: 3105-3111, 2005
21. Springall DR, Cadieux A, Oliveira H, Su H, Royston D, Polak JM: Retrograde tracing shows that CGRP-immunoreactive nerves of rat trachea and lung originate from vagal and dorsal root ganglia. *J Auton Nerv Syst* 20: 155-166, 1987
22. Tuder RM, Abman SH, Braun T, Capron F, Stevens T, Thistlethwaite PA, Haworth SG: Development and pathology of pulmonary hypertension. *J Am Coll Cardiol* 54: 3-9, 2009
23. Vaughan DJ, Brogan TV, Kerr ME, Deem S, Luchtel DL, Swenson ER: Contributions of nitric oxide synthase isozymes to exhaled nitric oxide and hypoxic pulmonary vasoconstriction in rabbit lungs. *Am J Physiol Lung Cell Mol Physiol* 284: 834-843, 2003
24. Voelkel NF, Quaife RA, Leinwand LA, Barst RJ, McGoon MD, Meldrum DR, Dupuis J, Long CS, Rubin LJ, Smart FW, Suzuki YJ, Gladwin M, Denholm EM, Gail DB: Right ventricular function and failure: Report of a National Heart, Lung, and Blood Institute Working Group on Cellular and Molecular Mechanisms of Right Heart Failure. *Circulation* 114: 1883-1891, 2006